Fam65b is a new transcriptional target of FOXO1 that regulates RhoA signaling for T lymphocyte migration

Pablo Rougerie,[*,†,‡,1,2] Quitterie Largeteau,[*,†,‡,1] Laura Megrelis,[*,†,‡,1] Florent Carrette,[*,†,‡,3] Thomas Lejeune,[*,†,‡,4] Lara Toffali,[§] Barbara Rossi,[§] Mahel Zeghouf,[¶] Jacqueline Cherfils,[¶] Gabriela Constantin,[§] Carlo Laudanna,[§] Georges Bismuth,[*,†,‡] Marianne Mangeney,[*,†,‡,5] and Jérôme Delon[*,†,‡,5,6]

[*] INSERM, U1016, Institut Cochin, Paris, France.

[†] CNRS, UMR8104, Paris, France.

[‡] Université Paris Descartes, Paris, France.

[§]Department of Pathology, Division of General Pathology, University of Verona, Verona, Italy.

[¶]Laboratoire d'Enzymologie et Biochimie Structurales, Centre National de la Recherche Scientifique, Centre de Recherche de Gif, Gif-sur-Yvette, France.

Present addresses:

[2]Albert Einstein College of Medicine, Bronx, NY, USA.

[3] The Scripps Research Institute, Department of Immunology and Microbial Science, La Jolla, California, USA.

[4] SBIGeM, CEA/Saclay, Gif-sur-Yvette, France.

[1]P.R., Q.L. and L.M. contributed equally to this work.

[5] M.M. and J.D. contributed equally to this work.

[6] Correspondence: jerome.delon@inserm.fr; Ph: (33)-1-40-51-66-40; Fax: (33)-1-40-51-65-55.

Running title: Identification of a FOXO1-induced RhoA down-modulator.

ABSTRACT

Forkhead box Os (FOXOs) transcription factors favor both T cell quiescence and trafficking through their control of the expression of genes involved in cell cycle progression, adhesion and homing. Here, we report that the product of the *fam65b* gene is a new transcriptional target of FOXO1 that regulates RhoA activity. We show that Fam65b binds the small GTPase RhoA *via* a non canonical domain and represses its activity by decreasing its GTP loading. As a consequence, Fam65b negatively regulates chemokine-induced responses such as adhesion, morphological polarisation and migration. Therefore, these results show the existence of a new functional link between FOXO1 and RhoA pathways, through which the FOXO1 target Fam65b tonically dampens chemokine-induced migration by repressing RhoA activity.

INTRODUCTION

Efficient T-cell adaptive immune responses take place in secondary lymphoid organs such as lymph nodes (LN). Thus, circulating T lymphocytes have to leave the blood stream to home in LN through high endothelial venules (HEVs) and perform their surveillance task. This motile behavior necessitates a tight control of expression of some cell surface proteins such as the adhesive molecules CD62L and LFA-1, and the CCR7 chemokine receptor (1). In addition, many signaling pathways responsible for profound alterations in T lymphocyte morphology are activated during this migratory process and during motility inside LN (2).

Using a large scale study of the genes that are specifically controlled by FOXO1 in human T cells, we have previously shown that FOXO1 regulates a much larger set of genes than previously expected. In addition to controlling a specific category of genes involved in T lymphocyte quiescence and survival, FOXO1 also controls expression of the CD62L and CCR7 homing receptors (3). These results have been largely confirmed in murine systems (reviewed in 4). However, no putative transcriptional targets of FOXO1 involved in the control of signals transduced downstream these homing receptors have been identified so far.

Here, we describe the function of a new gene controlled by FOXO1 called *fam65b* that fulfils such a function. In resting T cells, we report that Fam65b negatively regulates adhesion, polarisation and migration. Mechanistically, we show that Fam65b represses these responses by inhibiting RhoA activity, a GTPase particularly important for cell migration (5). This shows the existence of a novel and unsuspected link between FOXO1 and RhoA pathways. Taken together, our results demonstrate that Fam65b is a target gene of FOXO1 that regulates the triggering threshold of RhoA-dependent chemokine responses.

Materials and Methods

In silico *analysis*

The following publicly accessed databases were used: BLAST, UniGene, GeneCards, GeneAtlas, Clustal, Pfam, InterProScan, PSORT II Prediction, Panther and PROSITE. Accession numbers are: *fam65b* (UGID:1775160) (http://www.ncbi.nlm.nih.gov/UniGene/clust.cgi?ORG=Hs&CID=559459); Fam65b isoform 1 (Fam65b(1), 140 kDa, NP_055537.2); Fam65b isoform 2 (Fam65b(2), 85 kDa, NP_056948.2) (http://www.ncbi.nlm.nih.gov.gate2.inist.fr/protein?term=Fam65b).

qRT-PCR

Total RNA was prepared using RNeasy mini kit (Qiagen). cDNA was produced with the Advantage RT-for-PCR kit (Clontech Laboratories) using 1 µg of total RNA and random hexamer priming in a final volume of 20 µl. Real-time quantitative PCR was performed by using the LightCycler FastStart DNA Master plus SYBRGreen kit (Roche Diagnostics). Genes of interest were detected using primers that had been designed with the Oligo6 software (Molecular Biology Insights) and optimized to generate a single amplicon of 80–130 nucleotides. The sequences of the primers used in qRT-PCR experiments are the following: *ppia* (F): 5'- GGT GAC TTC ACA CGC CAT AAT G -3'; *ppia* (R): 5'- ACA AGA TGC CAG GAC CCG TAT -3'; *fam65b* (F): 5'-GCG GAG TTT AAC CTC AGC AG-3'; *fam65b* (R): 5'-CCT TCA GGT GTG ACT TTG GC-3'; *iso1*(F): 5'- GTC CCC TTC ACC CAA GT-3'; *iso1*(R): 5'- GGG TTC TCT GGC ATA TAA AAG-3'; *iso2*(F): 5'- CGC AAG AAT GCAT ACA AAC-3'; *iso2*(R): 5'- GAA GGC AGT TTG AGC GA-3'.

Luciferase assays

The FOXO1 enhancer in the *iso1* (130 650-131 815) and *iso2* promoter region (164 220-165 360) was amplified from human genomic DNA using the following set of primers: *iso1*-KpnI: 5'-ATACATGGTACCATGTTCCCTTTCGGCTAATGTCTCA-3' and *iso1*-BglII: 5'-ATGTATAGATCTGACGGCTCCTTGTCATGTCAGGGGC-3; *iso2*-KpnI: 5'-ATACATGGTACCGTCAAATTGAGTACAGAAAGAACAG-3' and *iso2*-BglII: 5'-ATGTATAGATCTCTCAAAGCTACGCGAAGCAGCTCAG-3'). DNA was amplified for 30 cycles (94°C 30 s, 68°C 30 s) in 2× buffer with 1.5 mM $MgCl_2$, 0.25 mM dNTPs, 0.5 µM each primer, 100 ng genomic DNA, and 5 U *pfx platinium* (Invitrogen) in a total volume of 50 µl. The amplified sample was digested with KpnI and BglII and introduced into the pGL3 vector (Promega) opened by the same enzymes. Jurkat T antigen cells ($5x10^6$/well) were co-transfected with Firefly luciferase reporter construct (5 µg), CMV-Renilla luciferase reporter construct (0.1 µg) and *FOXO1(3A)-GFP*. 24 h after transfection, cells were lysed in passive cell lysis buffer (500 µl) and luciferase activity was assayed using the Dual-Luciferase Reporter assay system (Promega) as *per* the manufacturer's instructions.

Constructs

The pEGFP-C3-RhoAN19 constructs was provided by M.R. Philips (New York University School of Medicine, USA). The FOXO1(3A)-GFP and FOXO1(3A,H215R)-GFP plasmids were previously described (3, 6). Lentiviral vectors TRIPiziE encoding GFP or FOXO1(3A)-GFP were described (3). Fam65b(2) was PCR-amplified using a V5-tagged Fam65b vector (7) as a template; the PCR fragment was then introduced into pEGFP-N1 vector (Clontech). Fam65b(1) was PCR-amplified using T lymphocyte cDNA as a template and similarly

introduced into pEGFP-N1. V5-tagged Fam65b(2) truncated mutants were described (7).

ChIP assays

JTag cells infected with lentiviral vectors encoding GFP or FOXO1(3A)-GFP were used three days later for some ChIP experiments performed with the Chromatin Immunoprecipitation (ChIP) assay kit (Millipore) according to the manufacturer's instructions. Anti-GFP and control irrelevant rabbit IgG were purchased from Abcam. DNA was extracted using a phenol/chloroform method. PCR reactions were conducted using the ampliTaq Gold kit with Gene Amp using the following parameters: 30 cycles (94°C 30 s, 58°C 1 min, 72°C 1.5 min) and the indicated primers (Supplemental Fig. 2B, C). Migration of PCR products was then performed with 2.5% agarose gels.

Yeast two-hybrid screen

Yeast two-hybrid screening was performed by Hybrigenics (Paris, France) using full-length Fam65b(2) as bait to screen a random-primed human $CD4^+$ $CD8^+$ thymocytes cDNA library.

Cells

Human PBT were purified from the blood of healthy donors as described (8). Jurkat T Ag and 293T cells were cultivated in complete RPMI medium.

DNA and RNAi transfections

293T cells were transfected with Lipofectamine2000 (Invitrogen) according to the manufacturer's instructions. 2.10^6 Jurkat T antigen cells were nucleofected with 5 µg DNA using the Amaxa system (Lonza) (kit V, program X-001). 5.10^6 PBT per cuvette were nucleofected with 10 µg DNA of the indicated construct using Amaxa and the U14 program.

For RNAi experiments, 2.10^6 PBT per cuvette were nucleofected with 2 µl of a 100 µM solution of OTP smartpool RNAi (Dharmacon) directed against human Fam65b or non-targeting sequences as a control. Cells were rested for 10 min in RPMI at 37 °C and then supplemented with complete RPMI medium containing human AB serum and 5 U/ml IL-7. Cells were then tested for functional experiments 3 days after nucleofection when the level of Fam65b knock-down was maximal.

Biochemistry

Protein expression levels of Fam65b were analysed by Western blot as described (8). Both Fam65b isoforms were revealed by immunoblotting with anti-Fam65b (Abnova). Other blotting antibodies were anti-RhoA (Cytoskeleton) and anti-β actin (Sigma) followed by goat-anti-mouse-HRP (BioRad) incubation and ECL revelation.

For pull-down assays, beads containing GST-tagged RhoA (Cytoskeleton) were incubated with 1 mM GDP or 0.2 mM GTPγS in the presence of 15 mM EDTA at 30 °C for 15 min and then locked in the GDP or GTPγS -bound conformation by supplementing 60 mM $MgCl_2$. They were then added to the cleared lysate of Fam65b-GFP -expressing 293T cells in the following buffer: 100 mM NaCl, 50 mM Tris-HCl (pH 7.4), 1% NP-40, 10% glycerol, 2 mM $MgCl_2$ in the presence of Complete protease inhibitors. For pull-down assays on PBT, 50.10^6 cells were stimulated with 200 ng/ml CCL19 for different times and the lysates were similarly submitted to a pull-down assay using 5 µg GST or GST-RhoA coated on glutathione beads. Alternatively, His-RhoA or His-RhoAL63 proteins (Cytoskeleton) were loaded on LiquiChip® Penta-His beads (Qiagen) according to the manufacturer's instructions and put in presence of GST-Fam65b(2) recombinant protein (Abnova) in PBS containing 1% BSA. All samples were then agitated for 1h, washed and processed as described above. Membranes were blotted with anti-GFP (living colors, Molecular Probes), anti-V5 (Invitrogen), anti-His

(Invitrogen), anti-Fam65b (Abnova) or anti-GST (Amersham) antibodies. Goat anti-mouse or anti-rabbit antibodies (BioRad) conjugated to HRP were then used and membranes were revealed by ECL.

RhoA activation assay

RhoA-GTP levels were measured using the G-LISA™ RhoA activation assay (Cytoskeleton). PBT stimulated or not with CCL19 (200 ng/ml) for 30 sec were lysed for 30 min with occasional stirring in the following lysis buffer in the presence of complete protease inhibitors: 50 mM Hepes, 1% Triton-X100, 0.5% deoxycholate, 0.05% SDS, 500 mM NaCl, 10 mM $MgCl_2$, 2 mM EGTA, 20 mM Benzamidine. Protein concentrations were quantified according to the manufacturer's recommendations. Equal amounts of proteins were added in triplicate to a 96-well plate coated with the RhoA binding domain of Rhotekin and incubated at 4 °C for 1 hour. Wells containing only some lysis buffer were used as blank samples. After washing, the amount of RhoA-GTP bound to each well was revealed by an anti-RhoA antibody followed by a secondary HRP-labeled antibody and detection of HRP. Signals were measured with a microplate spectrophotometer by quantifying absorbance at 490 nm.

Nucleotide Exchange Kinetics Assay

Nucleotide exchange activity on 2 µM of RhoA was measured with or without 2 µM of Dbs using a RhoGEF exchange assay kit (Cytoskeleton, Inc.) according to the manufacturer instructions, except that 6His-RhoA was produced in our laboratory (9). Fluorescence measurements were performed at 25 ˚C in a 384-well plate using a FlexStation 3 (Molecular Devices) with excitation and emission wavelengths of 360 and 440 nm, respectively. The exchange reaction was initiated by addition of Dbs, with or without 0.6 µM of recombinant Fam65b (Abnova) and monitored for 30 min. k_{obs} were calculated by fitting the fluorescence

changes to a single exponential, using the Prism 5 software (GraphPad Software, Inc.).

Flow cytometry

PBT were stimulated at 37 °C with 100 ng/ml CCL19 for different times, fixed with 4% paraformaldehyde for 10 min, permeabilised with 0.1% saponin and incubated with phalloidin-TRITC (Sigma). The F-actin content was then measured in each sample by flow cytometry using a FACScan (Becton Dickinson). JTag cells nucleofected with GFP, FOXO1-GFP, FOXO1(3A)-GFP or FOXO1(3A,H215R)-GFP were similarly processed for flow cytometry using an anti-Fam65b antibody (Santa Cruz).

Immunocytochemistry

JTag cells or PBT unstimulated or stimulated with 100 ng/ml CCL19 for different times, were fixed with 4% paraformaldehyde (PFA) for 10 mins, permeabilised with 0.1% Triton-X100 and incubated with a combination of phalloidin-Alexa-Fluor350 (Invitrogen), anti-moesin (C-15, Santa Cruz) and anti-Fam65b (Antibody Research, Inc. or Santa Cruz). Because we have confirmed that PFA fixation does not work for RhoA staining (10), anti-RhoA (26C4, Santa Cruz) immunofluorescence was performed using a 10% trichloroacetic acid (TCA) fixation method together with a P-ERM (Cell Signaling Technology) staining to localize the uropod. Unfortunately, Fam65b staining does not work with TCA fixation which precludes the possibility of performing a RhoA-Fam65b co-staining. DAPI or Hoechst stainings (blue) were used in some cases to stain the nucleus. Primary antibodies were revealed by biotin-, FITC- or Texas Red- conjugated anti-rabbit, anti-mouse or anti-goat IgG antibodies (Jackson ImmunoResearch). Streptavidin-Alexa fluor™ 568 (Invitrogen) was used to reveal secondary biotinylated antibodies. T lymphocytes were then allowed to sediment, mounted on glass coverslips using FluorSave™ Reagent (Calbiochem) and imaged by confocal microscopy.

Adhesion assays

For under-flow adhesion assays, CT or Fam65b KD T cells were resuspended at 10^6/ml in standard adhesion buffer (PBS, 1 mM $CaCl_2$, 1 mM $MgCl_2$, 10 % FCS, pH 7.2). Cellular adhesive interactions were studied in underflow conditions with the BioFlux 200 system (Fluxion Biosciences). A 48-well plate microfluidics was first co-coated overnight at room temperature with human E-selectin (5 µg/ml; R&D system) and human ICAM-1 (5 µg/ml; R&D system) in PBS. Before use, microfluidic channels were washed with PBS, coated with 2 µM CCL19 in PBS for 3 h at room temperature and the assay was done at a wall shear stress force of 2 dyne/cm^2. After extensive washing of channels with adhesion buffer, the behavior of interacting lymphocytes was recorded on digital drive with a fast CCD videocamera (25 frames/sec, capable of 1/2 subframe 20 msec recording) and analyzed subframe by subframe. Single areas of 0.2 mm^2 were recorded for at least 120 sec. Interactions of 20 msec or longer were considered significant and scored. Lymphocytes that remained firmly adhesive for at least 1 sec were considered fully arrested. Cells arrested for at least 1 sec or 10 sec were scored.

In vivo lymphocyte arrest on blood vessels endothelial cells was studied by intravital microscopy as described (11). Briefly, CT or Fam65b KD T cells (in DMEM without sodium bicarbonate supplemented with 20 mM HEPES, 5 % FCS, pH 7.1) were labelled with either CMFDA (1 min at 37 °C) or CMTMR (3 min at 37 °C). 15 x 10^6 labelled cells were injected i.v. in the tail vein of C57BL/6J mice. *In situ* video-microscopic analyses were carried out in Peyer's patches HEVs. Experiments were recorded on digital videotape with a high sensitive fast SIT videocamera (25 frames / sec). Cell behavior was analysed over a period of 20-30 min starting 2 min after i.v. injection. T lymphocytes that remained firmly arrested for at least 10 sec were scored.

Polarization

T cell polarization assays and the analysis of the 4 categories of morphological changes elicited by CCL19 stimulation were performed as described (12).

Migration

Nucleofected PBT were placed on the upper chamber of a 5-µm diameter transwell (Nunc). Different concentrations of CCL19 were put in the lower chamber and the cells were allowed to migrate for 3 hours. Lymphocytes that had reached the lower chamber were then harvested, put in a FACScan tube together with an equal amount of flow check fluorspheres (Beckman Coulter). The number of migrating cells was analysed by flow cytometry relative to the number of beads.

Statistics

Means +/- SE are shown when indicated. Statistically significant differences between groups were assessed with an unpaired Student's *t* test calculated with KaleidaGraph.

Results

Fam65b is induced by FOXO1

We initially identified *fam65b* as a major response gene of FOXO1 by microarray experiments in human T lymphocytes (3). Fam65b (Family with sequence similarity 65 member b) also called c6orf32, has two paralogs (Fam65a and Fam65c), all three molecules being well conserved from Zebra fish to humans (Supplemental Fig. 1A), especially in their N-terminal regions. In humans, this gene is located on chromosome 6 and encodes two mRNA isoforms that give rise to two proteins (Supplemental Fig. 1B). A UniGene search for the distribution of the transcripts indicated that *fam65b* mRNA levels are particularly high in blood cells and adult tissues of hematopoietic origin such as the secondary lymphoid organs (Supplemental Fig. 1C).

As presented in supplemental figure 2, the *fam65b* gene encodes two mRNA isoforms. To further characterize the regulation of Fam65b expression by FOXO1, we designed PCR primers amplifying specifically each isoform, and followed their expression in the Jurkat T cell line expressing a constitutively active nuclear form of FOXO1 (FOXO1(3A)). As shown in figure 1A as measured by qRT-PCR, Jurkat cells expressing FOXO1(3A) exhibited a 4.5 ± 0.1 and 6.5 ± 3 (mean ± S.E.M.) fold increase in Fam65b isoform 1 and isoform 2 transcript levels, respectively. The FOXO1(3A,H215R) mutant, which exhibits impaired DNA binding, induced only a marginal increase of 2 ± 0.1 for isoform 1 and 1.75 ± 0.35 for isoform 2 in transcript levels.

The two *fam65b* transcripts have their own promoters that have been identified using the Ensembl database (Supplemental Fig. 2A). To determine whether FOXO1 directly controlled *fam65b* gene transcription, we searched for evolutionary conserved FOXO1-binding site in the two *fam65b* promoters with the Genomatix program. We found one

putative FOXO1 site within the 500 bp of iso1 promoter region and four within iso2 that were conserved between mouse and human (Supplemental Fig. 2B, C). To further demonstrate that FOXO1 does indeed regulate Fam65b expression, luciferase reporter plasmids of *fam65b* were constructed for each promoter and co-transfected with FOXO1(3A) vector into Jurkat cells. The results showed that the luciferase activity of isoform 1 promoter (3.5 ± 0.4) and isoform 2 promoter (8.9 ± 0.9) was significantly increased by FOXO1(3A) (Fig. 1B). To investigate further whether FOXO1 directly binds these DNA elements, we used Jurkat cells transduced with FOXO1(3A) fused with GFP or GFP alone to perform chromatin immunoprecipitation experiments. For the promoter of isoform 1, a genomic fragment containing the FOXO1 site but not an irrelevant sequence is selectively enriched with anti-GFP antibody only in FOXO1(3A)-transduced cells (Fig. 1C). For the isoform 2 promoter, only the most proximal 5' fragment is detected with anti-GFP in FOXO1(3A)-transduced cells, demontrating that only this site is active in T lymphocytes for regulating isoform 2 expression by FOXO1. These findings demonstrate that the two isoforms of Fam65b are direct FOXO1 targets in T cells.

We next aimed at determining whether FOXO1 also increases Fam65b protein levels by transfecting Jurkat cells with different FOXO1-GFP constructs (FOXO1-GFP, FOXO1(A3)-GFP, FOXO1(3A,H215R)) or GFP alone. Fam65b levels were then measured by flow cytometry in the different cell populations discriminated by the expression of GFP. The results show that the constitutively active form of FOXO1 induces Fam65b expression whereas the wild type form of FOXO1 fails to trigger this expression (Fig. 1D). This is in accordance with its complete exclusion of the nucleus in this cellular model (Fig. 1E) due to the fact that Jurkat cells, that lack expression of the lipid phosphatase PTEN, have a tonic inactivation of wild-type FOXO1, even when it is overexpressed (3). As expected, the FOXO1(3A,H215R) molecule was poorly active as compared to the fully active FOXO1(A3)

mutant (Fig. 1D) despite its nuclear localization (Fig. 1E). Moreover, we show that Fam65b induced by active FOXO1 exhibits a cytosolic distribution (Fig. 1E).

Altogether, these results demonstrate that FOXO1 directly controls *fam65b* transcription and the expression of this protein in T lymphocytes.

Fam65b negatively regulates adhesion, polarization and migration upon chemokine stimulation

In unstimulated T cells, we and others have previously shown that FOXO1 controls the expression of CCR7 which binds the homeostatic chemokines CCL19 and CCL21 (3, 13). CCR7 is crucial for lymph node homing (14) or during intra-nodal motility (15-17). Because we demonstrate here that FOXO1 also controls Fam65b expression in resting T lymphocytes, we next tested whether Fam65b plays a role in CCL19 responses.

Using a RNAi approach (Supplemental Fig. 3A), we first tested whether Fam65b plays a role in T cell adhesion upon CCL19 stimulation. Adhesion under flow upon chemokine stimulation elicits a rapid inside-out mechanism of integrin activation that supports a quick cell arrest that might be followed by additional mechanisms to stabilize adhesion (18). Under-flow adhesion assays were conducted for control (CT) and Fam65b knocked-down (KD) T lymphocytes visualised in microfluidic channels coated with CCL19, E-selectin and ICAM-1. The behavior of CT and KD T cells is quantified in Fig. 2A. KD T cells have a lower tendency to exhibit rolling (Fig. 2A, *left*) and reciprocally show an increased propensity to adhere briefly (Fig. 2A, *middle*) or more stably (Fig. 2A, *right*). We next aimed at evaluating the adhesive role of Fam65b in the complexity of an *in vivo* situation under physiological shear stress forces. We used a validated xenobiotic setting that consists in imaging the microcirculation of human T cells in the Peyer's patches HEVs of anesthetized mice by intravital microscopy (11). In these conditions, Fam65b depletion increases the percentage of

stably arrested T lymphocytes (Fig. 2B). Therefore, Fam65b negatively regulates T lymphocyte adhesion, both *in vitro* and *in vivo*.

We then analysed the capacity of Fam65b KD cells to polarize morphologically upon CCL19 stimulation as described (12). Interestingly, even without any chemokine stimulation, Fam65b KD cells tend to spontaneously polarize slightly more than control cells (Fig. 2C). After CCL19 stimulation, twice as many KD cells progressed toward the fully polarized stage compared to control cells (Fig. 2C).

As polarity establishment is considered to be a prerequisite for optimal migration (19, 20), we next aimed at testing a role for Fam65b in T cell migration. We first observed that in absence of chemokine stimulation, KD cells are more prone to migrate spontaneously (Fig. 2D). This phenomenon was more amplified at sub-optimal CCL19 concentration, as the sole Fam65b depletion was able to turn immobile cells into lymphocytes efficiently migrating 4 times above the baseline level (Fig. 2D*, middle*), most likely due to the higher fraction of polarized cells.

Altogether, these results show that Fam65b negatively regulates the threshold for T cell adhesion, polarisation and migration.

Fam65b is a new partner of RhoA

In our initial attempt to delineate the signaling pathways regulated by Fam65b, several independent observations pointed toward the RhoA GTPase. (i) A remarkable aspect is that the T cell functions reported above, in which Fam65b has an inhibitory role, have been reported to depend on RhoA activity, whereas actin polymerization in primary T lymphocytes is controlled neither by RhoA nor by Fam65b (Supplemental Fig. 3B) (21-25). (ii) An *in silico* approach using Panther classification system for phylogenetically related proteins identified Fam65b as a molecule related to the RhoA partner PKN (26, 27) (PTHR15829).

(iii) A yeast two-hybrid screen set up for identifying Fam65b partners identified the small GTPase RhoA as a possible candidate for Fam65b binding.

In order to confirm this interaction, we realized a series of pull-down assays. As shown in figure 3A and B, both Fam65b isoforms strongly interact with RhoA in an inactive GDP-bound form as well as an active GTP-bound form. Titering down the amount of RhoA-GDP or RhoA-GTP in this assay still maintained similar binding to Fam65b (Fig. 3C), irrespective of the type of nucleotide loaded. Association of Fam65b with wild-type RhoA or the constitutively active mutant RhoAL63 was also detected purely *in vitro* with recombinant proteins, demonstrating a direct association between Fam65b and RhoA (Fig. 3D).

We next attempted to identify the Fam65b region responsible for RhoA binding. A series of truncated Fam65b mutants was tested in a pull-down assay. N-terminal deletion of the first 54 amino acids maintained the ability of this mutant to bind RhoA (Fig. 3E). However, removal from amino acid 113 and beyond completely abrogated RhoA interaction. Conversely, deletion of the last 101 amino acids did not affect binding to RhoA. We conclude that Fam65b binds RhoA through the 54-113 region of Fam65b.

In addition, this interaction between RhoA and endogenous Fam65b in the lysates of primary human T cells was detected (Fig. 3F). Importantly, whereas a strong association was observed in un-stimulated T lymphocytes, it was transiently decreased upon CCL19 stimulation. This result indicates that CCL19 signaling frees RhoA from Fam65b binding.

Fam65b inhibition of migration depends on RhoA binding

We next aimed at determining whether the Fam65b-RhoA interaction could account for the effect of Fam65b on T cell migration.

We first checked whether RhoA controls T cell migration as described for many other cell types (5). This was verified in our system for T cell migration elicited by CCL19

signaling using a dominant negative mutant of RhoA. The inhibition of RhoA activity elicited a strong inhibition of T cell migration (Fig. 4A). Overexpression of full-length Fam65b also inhibited T cell migration whereas the Δ113 mutant, that does not bind RhoA, did not (Fig. 4B). This result confirms the inhibitory effect of Fam65b on chemokine-induced migration, and unveils the requirement for the RhoA binding region of the protein for this inhibition.

Fam65b inhibits RhoA activity

The functional effects of Fam65b on migration could thus arise from an inhibition of the activity of its partner RhoA. To further test this hypothesis, we directly measured the content of active GTP-bound RhoA in Fam65b-KD or control cells. The results show that resting KD cells had a higher content in RhoA-GTP that did not increase substantially after chemokine stimulation contrary to control T cells (Fig. 5A). Thus, Fam65b acts as a factor that tonically inhibits the RhoA pathway by decreasing the T cell RhoA-GTP content.

In order to delineate the molecular mechanism by which Fam65b inhibits RhoA activity, we also performed an *in vitro* nucleotide exchange assay to measure the kinetics of RhoA GTP loading by the Guanine nucleotide Exchange Factor (GEF) domain of the RhoGEF Dbs in the presence of Fam65b. In a solution containing fluorescent GTP, we could observe a slow and passive loading of GTP on RhoA that was largely independent of the presence of Fam65b (Fig. 5B, *left*). Addition of recombinant Dbs accelerated GTP loading as expected. However, the presence of Fam65b slowed down the exchange rate of Dbs on RhoA, as shown by a 5-times reduction in the k_{obs} value (Fig. 5B, *right*).

Therefore, we conclude that Fam65b down-modulates the exchange reaction that GEFs perform on RhoA and consequently dampens levels of active RhoA in T cells.

Discussion

Here, we report that the transcription factor FOXO1 does not only regulate cell growth and the expression of homing receptors as previously demonstrated (3), but also controls an important signaling pathway involved in T cell migration. Indeed, we have found that Fam65b, a phylogenetically well-conserved protein, is induced by FOXO1 and represses RhoA activity providing a new and unexpected bridge between the FOXO1 and RhoA pathways in order to modulate T cell motility.

It is puzzling to note that FOXO1 seems to have opposite effects on motility as it induces expression of CD62L and CCR7 that favor homing and expression of Fam65b that negatively regulates migration. It is not clear at the moment whether this paradox constitutes for FOXO1 a way of finely regulating motility. Alternatively, our *in vivo* data demonstrate a negative role for Fam65b in T cell adhesion to HEVs. This could allow FOXO1 to indirectly promote homing again by avoiding T cells to exhibit too strong adhesive properties that would maintain them otherwise stuck onto blood vessels. The use of a mouse model deficient for Fam65b should allow us to test this possibility.

We show that Fam65b markedly affects adhesion, polarization and migration upon chemokine exposure although it does so without exhibiting obvious changes in its subcellular localization (Supplemental Fig. 4A). This is in agreement with the fact that Fam65b can interact with RhoA independently of the type of nucleotide it bears and that the total pool of RhoA is distributed on both sides of a polarised T cell (Supplemental Fig. 4B) (10). We report here that Fam65b exerts a tonic inhibition on RhoA activity. Together with other necessary signaling pathways triggered upon chemokine stimulation, the depletion in Fam65b is thus likely to account for the advantage exhibited by the KD cells to polarize and migrate.

Interestingly, we also show that Fam65b-RhoA interaction decreases upon CCL19 stimulation, suggesting that the loss of Fam65b control on RhoA activity is likely to allow for RhoA activation in normal conditions.

Fam65b is an unexpected regulator of RhoA. Indeed, it does not contain any known consensus domain found in typical RhoA interactants such as GAP (GTPase Activating Protein) and GEF proteins. It does not present any sequence similarity with GDI (Guanine nucleotide Dissociation Inhibitors) proteins either. In addition, as effectors can discriminate between the GDP- and GTP-bound forms of Rho GTPases, Fam65b does not belong to this class of Rho partners. Interestingly, previous papers have reported possible new mechanisms for RhoA regulation. The unrelated F11L (28) and Memo (29) proteins that do not contain any canonical domain of interaction with RhoA were indeed described as RhoA partners and regulators. Although the three proteins do not share any obvious sequence identity, these results indicate that RhoA activity can be controlled by thus far unrecognized mechanisms. We show here that Fam65b inhibits the exchange reaction performed by GEFs on RhoA. It would be interesting to determine whether these three non canonical RhoA partners, i.e. F11L, Memo and Fam65b, share a similar regulatory mechanism on RhoA.

Fam65b has previously been shown to be up-regulated during placenta and muscle cell differentiation and to induce membrane protrusions necessary for cell-cell fusion (7, 30, 31). In fact, it is the 54-113 portion of the protein that is required for this morphological effect in myoblasts (7). Interestingly, we show that this particularly well conserved region related to PKN and predicted to display a coiled-coil structure is necessary to bind RhoA, suggesting that the effect of Fam65b on myoblast fusion may depend on its ability to interact with RhoA and to inhibit its activity. Consistent with this model, others have shown that a decrease in RhoA-GTP content was indispensable to allow myoblast fusion (32). Therefore, we consider most likely that Fam65b behaves as an inducible repressor of RhoA activity to allow cell-cell

fusion during muscle or placenta formation is most likely.

In conclusion, we have identified here a new RhoA down-modulator whose expression is tightly controlled by FOXO1. Although our data have been obtained in T lymphocytes, the mechanisms uncovered in these cells may be of much wider significance in other cell types for contributing to other cell-specific functions. We have shown that Fam65b acts as a brake for T cell migration, and therefore represents a new target by which FOXO1 can regulate motile processes.

Acknowledgements

We thank E. Gussoni and M.R. Philips for providing reagents or mice; F. Campo-Paysaa for help with the phylogeny analysis; R.N. Germain, E. Gussoni, A. Trautmann, C. Randriamampita, E. Donnadieu and C. Charvet for discussions and critical reading of the manuscript.

Funding support

This work was supported by Inserm, CNRS and Ligue Nationale contre le Cancer; G.C. was supported by the European Research Council grant NEUROTRAFFICKING 261079; P.R., Q.L. and L.M. were supported by fellowships from the Ministry of Research and Higher Education. F.C. was supported by a fellowship from Association pour la Recherche sur le Cancer.

Disclosures

The authors have no financial conflicts of interest.

References

1. Campbell, D. J., C. H. Kim, and E. C. Butcher. 2003. Chemokines in the systemic organization of immunity. *Immunol Rev* 195:58-71.
2. Cahalan, M. D., and I. Parker. 2008. Choreography of cell motility and interaction dynamics imaged by two-photon microscopy in lymphoid organs. *Annu Rev Immunol* 26:585-626.
3. Fabre, S., F. Carrette, J. Chen, V. Lang, M. Semichon, C. Denoyelle, V. Lazar, N. Cagnard, A. Dubart-Kupperschmitt, M. Mangeney, et al. 2008. FOXO1 regulates L-Selectin and a network of human T cell homing molecules downstream of phosphatidylinositol 3-kinase. *J Immunol* 181:2980-2989.
4. Carrette, F., S. Fabre, and G. Bismuth. 2009. FOXO1, T-cell trafficking and immune responses. *Adv Exp Med Biol* 665:3-16.
5. Ridley, A. J., M. A. Schwartz, K. Burridge, R. A. Firtel, M. H. Ginsberg, G. Borisy, J. T. Parsons, and A. R. Horwitz. 2003. Cell migration: integrating signals from front to back. *Science* 302:1704-1709.
6. Fabre, S., V. Lang, J. Harriague, A. Jobart, T. G. Unterman, A. Trautmann, and G. Bismuth. 2005. Stable activation of phosphatidylinositol 3-kinase in the T cell immunological synapse stimulates Akt signaling to FOXO1 nuclear exclusion and cell growth control. *J Immunol* 174:4161-4171.
7. Yoon, S., M. J. Molloy, M. P. Wu, D. B. Cowan, and E. Gussoni. 2007. C6ORF32 is upregulated during muscle cell differentiation and induces the formation of cellular filopodia. *Dev Biol* 301:70-81.
8. Faure, S., L. I. Salazar-Fontana, M. Semichon, V. L. Tybulewicz, G. Bismuth, A. Trautmann, R. N. Germain, and J. Delon. 2004. ERM proteins regulate cytoskeleton relaxation promoting T cell-APC conjugation. *Nat Immunol* 5:272-279.

9. Bouquier, N., S. Fromont, J. C. Zeeh, C. Auziol, P. Larrousse, B. Robert, M. Zeghouf, J. Cherfils, A. Debant, and S. Schmidt. 2009. Aptamer-derived peptides as potent inhibitors of the oncogenic RhoGEF Tgat. *Chem Biol* 16*:*391-400.

10. Takesono, A., S. J. Heasman, B. Wojciak-Stothard, R. Garg, and A. J. Ridley. 2010. Microtubules regulate migratory polarity through Rho/ROCK signaling in T cells. *PLoS ONE* 5*:*e8774.

11. Bolomini-Vittori, M., A. Montresor, C. Giagulli, D. Staunton, B. Rossi, M. Martinello, G. Constantin, and C. Laudanna. 2009. Regulation of conformer-specific activation of the integrin LFA-1 by a chemokine-triggered Rho signaling module. *Nat Immunol* 10*:*185-194.

12. Real, E., S. Faure, E. Donnadieu, and J. Delon. 2007. Cutting edge: Atypical PKCs regulate T lymphocyte polarity and scanning behavior. *J Immunol* 179*:*5649-5652.

13. Kerdiles, Y. M., D. R. Beisner, R. Tinoco, A. S. Dejean, D. H. Castrillon, R. A. DePinho, and S. M. Hedrick. 2009. Foxo1 links homing and survival of naive T cells by regulating L-selectin, CCR7 and interleukin 7 receptor. *Nat Immunol* 10*:*176-184.

14. Gunn, M. D., K. Tangemann, C. Tam, J. G. Cyster, S. D. Rosen, and L. T. Williams. 1998. A chemokine expressed in lymphoid high endothelial venules promotes the adhesion and chemotaxis of naive T lymphocytes. *Proc Natl Acad Sci U S A* 95*:*258-263.

15. Asperti-Boursin, F., E. Real, G. Bismuth, A. Trautmann, and E. Donnadieu. 2007. CCR7 ligands control basal T cell motility within lymph node slices in a phosphoinositide 3-kinase-independent manner. *J Exp Med* 204*:*1167-1179.

16. Okada, T., and J. G. Cyster. 2007. CC chemokine receptor 7 contributes to Gi-dependent T cell motility in the lymph node. *J Immunol* 178*:*2973-2978.

17. Worbs, T., T. R. Mempel, J. Bolter, U. H. von Andrian, and R. Forster. 2007. CCR7 ligands stimulate the intranodal motility of T lymphocytes in vivo. *J Exp Med* 204*:*489-495.

18. Alon, R., and M. L. Dustin. 2007. Force as a facilitator of integrin conformational changes during leukocyte arrest on blood vessels and antigen-presenting cells. *Immunity* 26*:*17-27.

19. Krummel, M. F., and I. Macara. 2006. Maintenance and modulation of T cell polarity. *Nat Immunol* 7*:*1143-1149.

20. Thelen, M., and J. V. Stein. 2008. How chemokines invite leukocytes to dance. *Nat Immunol* 9:953-959.

21. Cantrell, D. A. 2003. GTPases and T cell activation. *Immunol Rev* 192:122-130.

22. Giagulli, C., E. Scarpini, L. Ottoboni, S. Narumiya, E. C. Butcher, G. Constantin, and C. Laudanna. 2004. RhoA and ζ PKC control distinct modalities of LFA-1 activation by chemokines: critical role of LFA-1 affinity triggering in lymphocyte in vivo homing. *Immunity* 20:25-35.

23. Vielkind, S., M. Gallagher-Gambarelli, M. Gomez, H. J. Hinton, and D. A. Cantrell. 2005. Integrin regulation by RhoA in thymocytes. *J Immunol* 175:350-357.

24. Pasvolsky, R., V. Grabovsky, C. Giagulli, Z. Shulman, R. Shamri, S. W. Feigelson, C. Laudanna, and R. Alon. 2008. RhoA is involved in LFA-1 extension triggered by CXCL12 but not in a novel outside-in LFA-1 activation facilitated by CXCL9. *J Immunol* 180:2815-2823.

25. Rougerie, P., and J. Delon. 2012. Rho GTPases: Masters of T lymphocyte migration and activation. *Immunol Lett* 142:1-13.

26. Amano, M., H. Mukai, Y. Ono, K. Chihara, T. Matsui, Y. Hamajima, K. Okawa, A. Iwamatsu, and K. Kaibuchi. 1996. Identification of a putative target for Rho as the serine-threonine kinase protein kinase N. *Science* 271:648-650.

27. Watanabe, G., Y. Saito, P. Madaule, T. Ishizaki, K. Fujisawa, N. Morii, H. Mukai, Y. Ono, A. Kakizuka, and S. Narumiya. 1996. Protein kinase N (PKN) and PKN-related protein rhophilin as targets of small GTPase Rho. *Science* 271:645-648.

28. Valderrama, F., J. V. Cordeiro, S. Schleich, F. Frischknecht, and M. Way. 2006. Vaccinia virus-induced cell motility requires F11L-mediated inhibition of RhoA signaling. *Science* 311:377-381.

29. Zaoui, K., S. Honore, D. Isnardon, D. Braguer, and A. Badache. 2008. Memo-RhoA-mDia1 signaling controls microtubules, the actin network, and adhesion site formation in migrating cells. *J Cell Biol* 183:401-408.

30. Dakour, J., H. Li, and D. W. Morrish. 1997. PL48: a novel gene associated with cytotrophoblast and lineage-specific HL-60 cell differentiation. *Gene* 185*:*153-157.

31. Hirayama, E., and J. Kim. 2008. Identification and characterization of a novel neural cell adhesion molecule (NCAM)-associated protein from quail myoblasts: relationship to myotube formation and induction of neurite-like protrusions. *Differentiation* 76*:*253-266.

32. Charrasse, S., F. Comunale, Y. Grumbach, F. Poulat, A. Blangy, and C. Gauthier-Rouviere. 2006. RhoA GTPase regulates M-cadherin activity and myoblast fusion. *Mol Biol Cell* 17*:*749-759.

FIGURE LEGENDS

FIGURE 1. Fam65b expression is controlled by FOXO1. (**A**) Jurkat cells transduced with GFP, FOXO1(3A)-GFP or FOXO1(3A, H215R)-GFP were analyzed 48 hrs later for *fam65b* isoform 1 or 2 transcript levels by qRT-PCR. Data are from three independent experiments. (**B**) Jurkat cells were co-transfected with a construct encoding FOXO1(3A)-GFP together with a luciferase reporter plasmid containing the putative FOXO1 enhancer in *fam65b* isoform 1 or 2 promoters and an internal *Renilla* luciferase reporter construct driven by the CMV promoter. 24 h post transfection, cells were lysed and *Firefly* and *Renilla* luciferase activities were measured. Data are shown as means of two independent experiments conducted in triplicate. (**C**) Chromatin proteins in Jurkat cells infected with GFP (control) or FOXO1(3A)-GFP were cross-linked to DNA and immunoprecipitated using anti-GFP or non immune rabbit IgG control. Eluted DNAs were diluted for PCR and amplified DNA fragments using specific primers (supplemental Fig. 2) were resolved on gel. (**D**) Flow cytometry analysis of Fam65b expression in Jurkat cells transfected with plasmids encoding GFP, FOXO1-GFP, FOXO1(3A)-GFP or FOXO1(3A,H215R)-GFP. Left: examples of dot plots showing the GFP expression levels as a function of Fam65b expression. Top right: Overlays of Fam65b expression gated in cells expressing GFP (red line), FOXO1-GFP (orange line), active FOXO1(3A)-GFP (green line) and active FOXO1(3A,H215R)-GFP (blue line). Bottom right: Mean fluorescence intensities of Fam65b expression in the GFP^+ gate of the different transfectants (means +/- SE from six independent experiments). (**E**) Subcellular localization of the different FOXO1 mutants in Jurkat cells. The following stainings are shown: GFP (green), Hoechst (blue) and Fam65b (red). Examples of representative cells are shown.

FIGURE 2. Fam65b inhibits T cell adhesion, polarization and migration upon chemokine stimulation. (**A**) Under-flow adhesion to ICAM-1 was tested in PBT transfected with control (CT) or Fam65b (KD) RNAi. The % of cells exhibiting rolling (*left*), or arrest for at least 1 sec (*middle*) or 10 sec (*right*) is shown. Means +/- SE from seven independent experiments. (**B**) The % of control (CT) or Fam65b-depleted (KD) PBT that arrested at least 10 sec on Peyer's patches HEVs *in vivo* were quantified (means +/- SE from ten microscopic fields obtained in four mice). (**C**) PBT transfected with control (CT, left) or Fam65b (KD, right) RNAi were stimulated or not with 100 ng/ml CCL19 for 8 mins, fixed and stained for F-actin. Each cell was scored into one of the four categories previously described (12): weak homogenous actin (black), mislocalized actin (white), polarized actin (light grey) and fully polarized with a uropod (dark grey). For each category, one example of the F-actin staining depicted with an inverted black and white scale is shown as an illustration. One example out of three experiments is shown. (**D**) PBT transfected with CT or Fam65b (KD) RNAi were tested for migration to different concentrations of CCL19 in a 3-hour transwell assay. One representative experiment out of three is presented.

FIGURE 3. Fam65b interacts with RhoA. Lysates from 293T cells transfected with Fam65b(1)-GFP (**A**) or Fam65b(2)-GFP (**B**) were subjected to a pull-down assay using beads bearing GST alone or 8 µg GST-RhoA loaded with GDP or GTPγS. wcl: whole cell lysate. (**C**) The lysate from 293T cells transfected with Fam65b(2)-GFP was incubated in a pull-down assay with 9, 3 or 1 µg GST-RhoA beads loaded with GDP or GTPγS. The RhoA-Fam65b association was tested by Western blot in the different conditions. (**D**) Human recombinant Fam65b(2) tagged with GST was added to beads loaded with no protein, His-RhoA (28 kD) or His-RhoAL63 (22 kD). Direct protein-protein interaction was analysed by

pull-down assay. Note that both recombinant RhoA proteins have slightly different molecular weight due to a small irrelevant amino acid stretch present between the His tag and the RhoA sequence of the wild type protein. (**E**) Left panel: The deletion mutants of Fam65b(2) are schematically represented. Right panel: Lysates from 293T cells transfected with Fam65b(2)-V5 FL (Full Length) or different deletion mutants in N- or C-terminal were submitted to a pull-down assay using GST-RhoA beads. For each transfectant, the first lane shows the wcl fraction and the second lane shows the amount of Fam65b(2) FL or mutant bound to RhoA. Each panel shows a representative experiment of at least three independent assays. (**F**) Lysates from PBT stimulated for different times with 200 ng/ml CCL19 were submitted to a pull-down assay using GST or GST-RhoA beads (top two panels). Fam65b in the whole cell lysate fraction is shown as a loading control (bottom panel). One experiment representative of three independent ones is shown.

FIGURE 4. The role of Fam65b in T cell migration depends on RhoA binding. (**A**) PBT transfected with GFP or GFP-RhoAN19 were tested as described previously in a transwell assay. The percentages of migratory T cells were normalized to the GFP-transfected population in each experiment set to 100. Data are from two independent experiments (**p*=0.039). (**B**) PBT transfected with empty vector (EV), full-length (FL) Fam65b(2) or Nt-Fam65b(2)Δ113 (Δ113) were similarly tested in a migration assay. Data obtained for each condition was normalised to the migration index obtained in EV-transfected T cells set to 100. Data are from eight donors (**p*=0.02; ***p*=0.005).

FIGURE 5. Fam65b inhibits RhoA activity. (**A**) PBT transfected with CT or Fam65b (KD) RNAi were stimulated or not with 200 ng/ml CCL19 for 30 sec. The active RhoA-GTP content was measured for each condition in triplicate by the G-LISA™ method. Data from

three independent experiments are shown (n.s.: not significant; **p=0.0317; ***p=0.0075). (**B**) Recombinant RhoA and Fam65b were placed alone or in combination in wells of a 384-well plate. Recombinant Dbs was then added and the plate was put in a FlexStation to read the evolution of RhoA GTP loading by fluorescence (*left*). Means +/- SE of k_{obs} values for RhoA+Dbs (n=8) or RhoA+Dbs+Fam65b (n=6) (*right*) (*p=0.014).

Figure 1

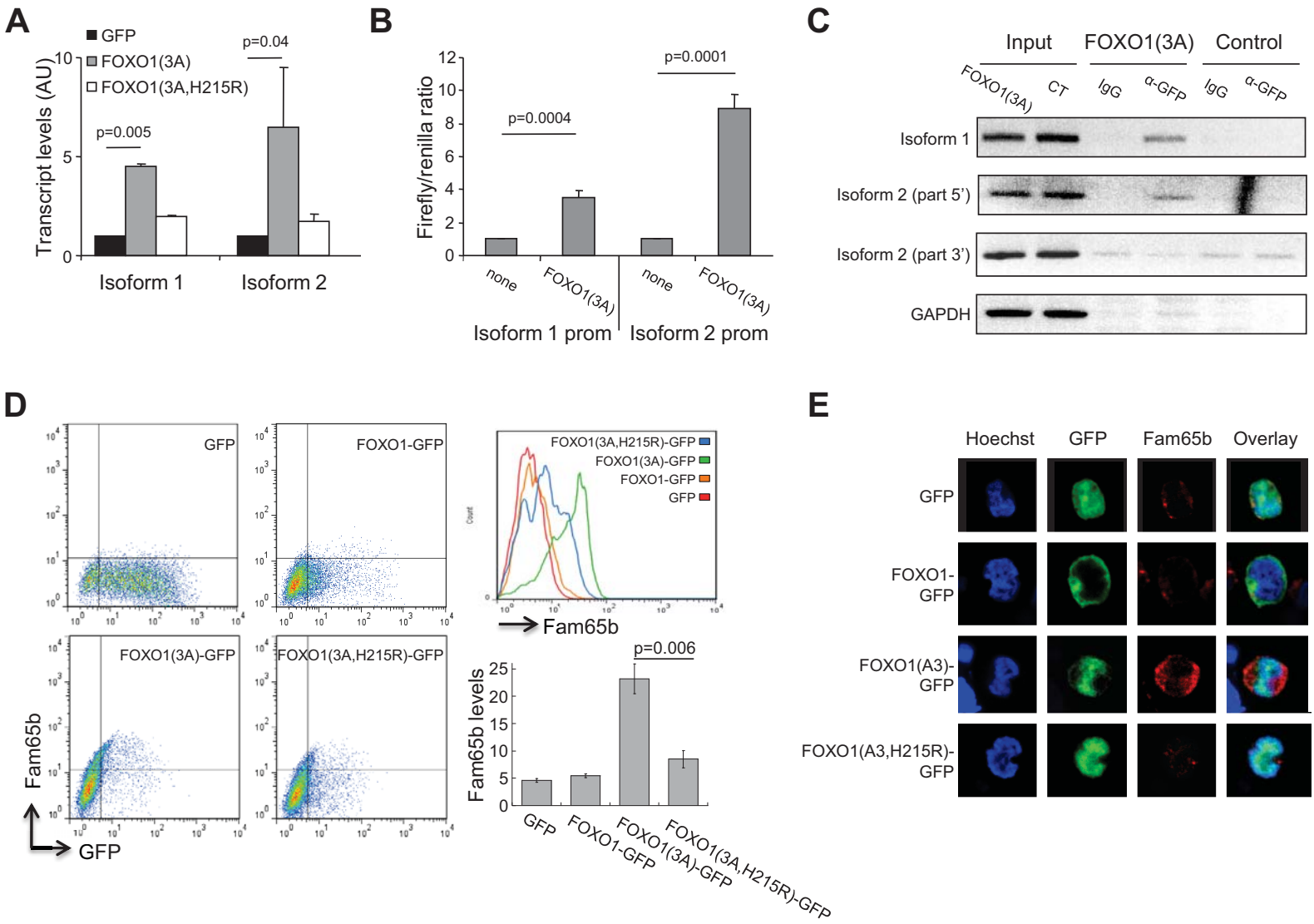
A
GFP
FOXO1(3A)
FOXO1(3A,H215R)
Transcript levels (AU)
p=0.005
p=0.04
Isoform 1
Isoform 2
B
Firefly/renilla ratio
p=0.0004
p=0.0001
none
FOXO1(3A)
Isoform 1 prom
Isoform 2 prom
C
Input
FOXO1(3A)
Control
FOXO1(3A)
CT
IgG
α-GFP
Isoform 1
Isoform 2 (part 5')
Isoform 2 (part 3')
GAPDH
D
GFP
FOXO1-GFP
FOXO1(3A)-GFP
FOXO1(3A,H215R)-GFP
Fam65b
GFP
FOXO1(3A,H215R)-GFP
FOXO1(3A)-GFP
FOXO1-GFP
GFP
Fam65b levels
p=0.006
E
Hoechst
GFP
Fam65b
Overlay
GFP
FOXO1-GFP
FOXO1(A3)-GFP
FOXO1(A3,H215R)-GFP

Figure 2

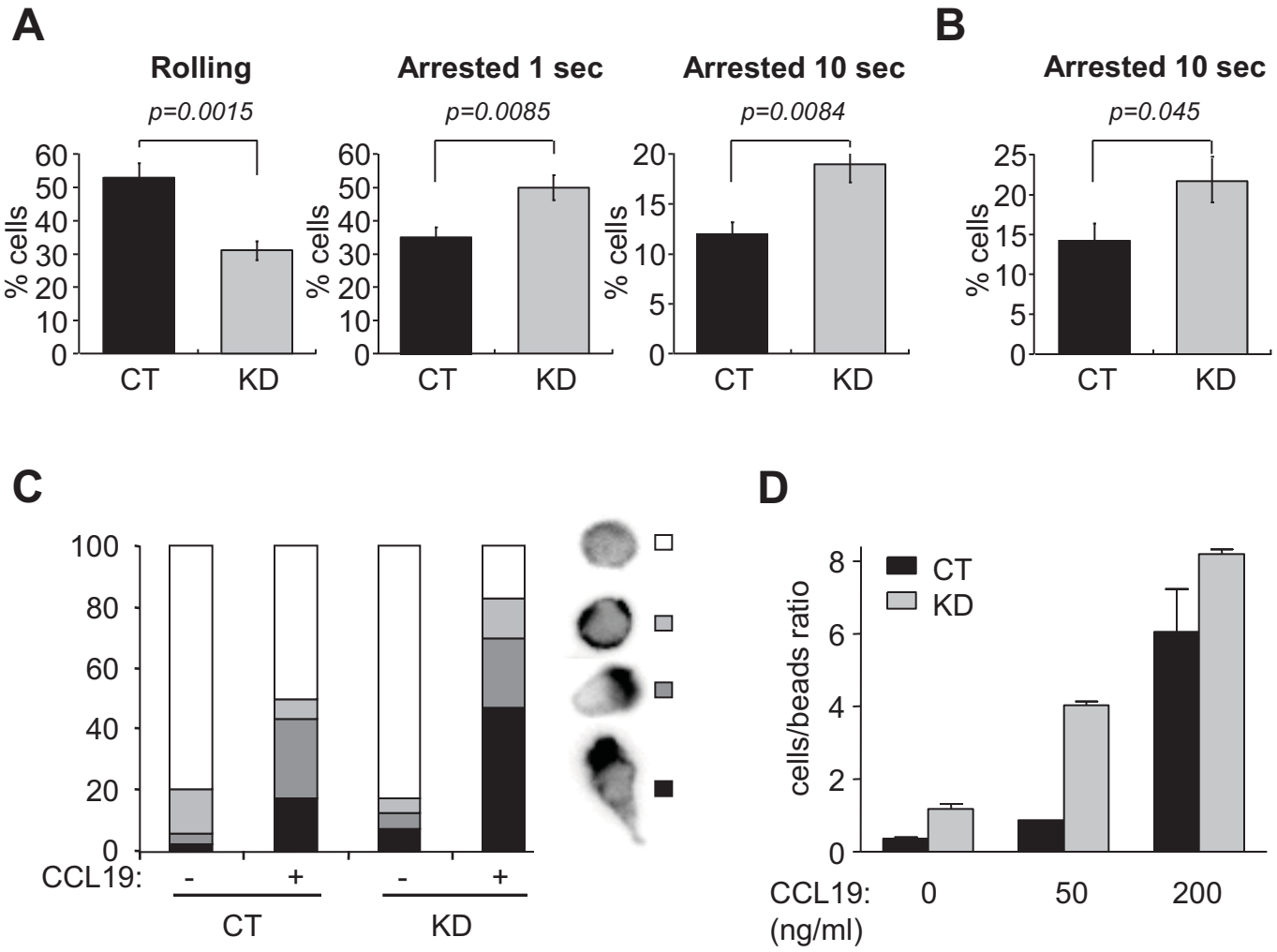
A
Rolling
p=0.0015
% cells
CT
KD
Arrested 1 sec
p=0.0085
Arrested 10 sec
p=0.0084
B
Arrested 10 sec
p=0.045
C
CCL19:
D
cells/beads ratio
CT
KD
CCL19: (ng/ml)
0
50
200

Figure 3

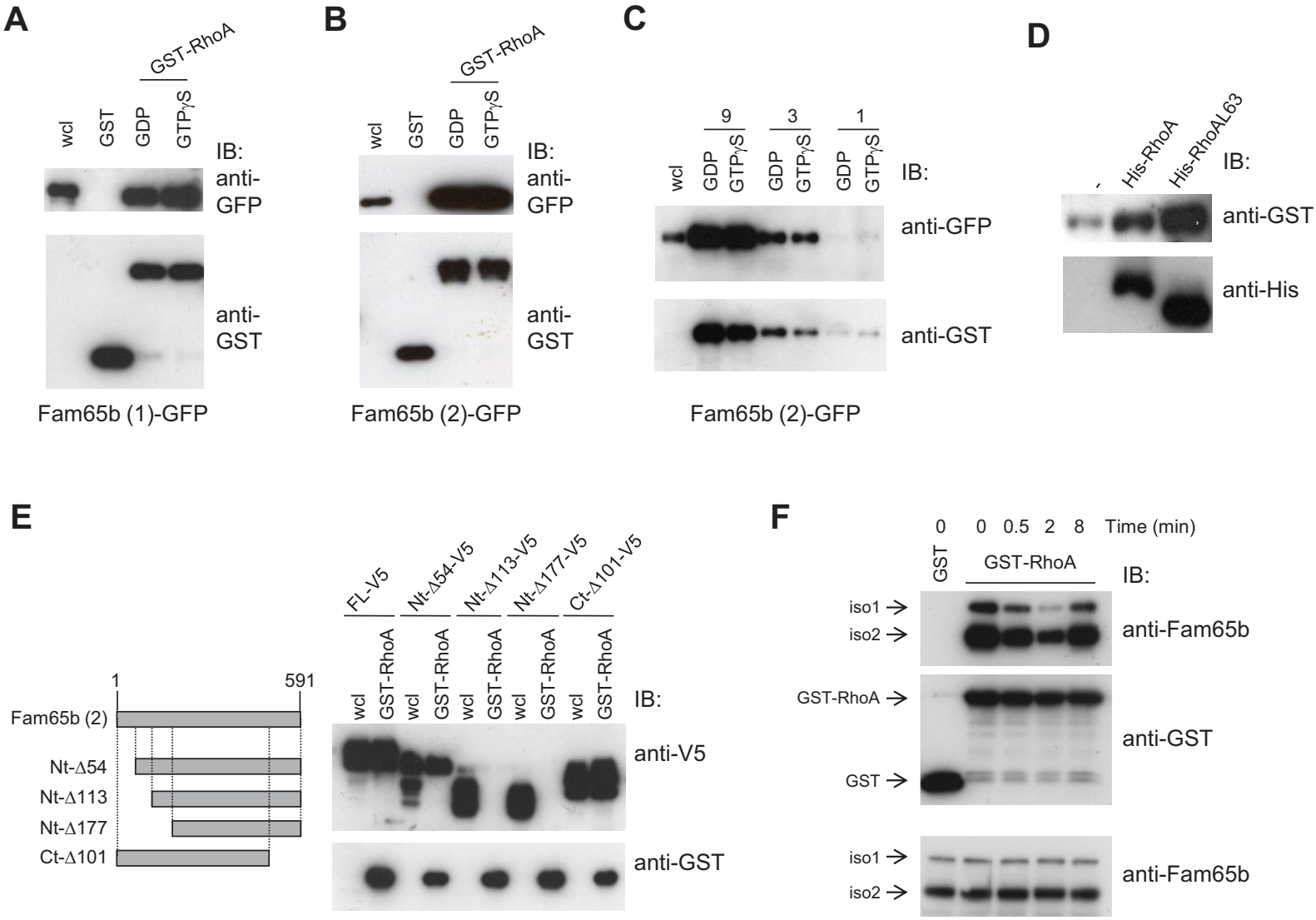
A
GST-RhoA
wcl
GST
GDP
GTPγS
IB:
anti-GFP
anti-GST
Fam65b (1)-GFP
B
GST-RhoA
wcl
GST
GDP
GTPγS
IB:
anti-GFP
anti-GST
Fam65b (2)-GFP
C
9
3
1
wcl
GDP
GTPγS
GDP
GTPγS
GDP
GTPγS
IB:
anti-GFP
anti-GST
Fam65b (2)-GFP
D
His-RhoA
His-RhoAL63
IB:
anti-GST
anti-His
E
1
591
Fam65b (2)
Nt-Δ54
Nt-Δ113
Nt-Δ177
Ct-Δ101
FL-V5
Nt-Δ54-V5
Nt-Δ113-V5
Nt-Δ177-V5
Ct-Δ101-V5
wcl
GST-RhoA
IB:
anti-V5
anti-GST
F
0
0
0.5
2
8
Time (min)
GST
GST-RhoA
IB:
iso1
iso2
anti-Fam65b
GST-RhoA
GST
anti-GST
iso1
iso2
anti-Fam65b

Figure 4

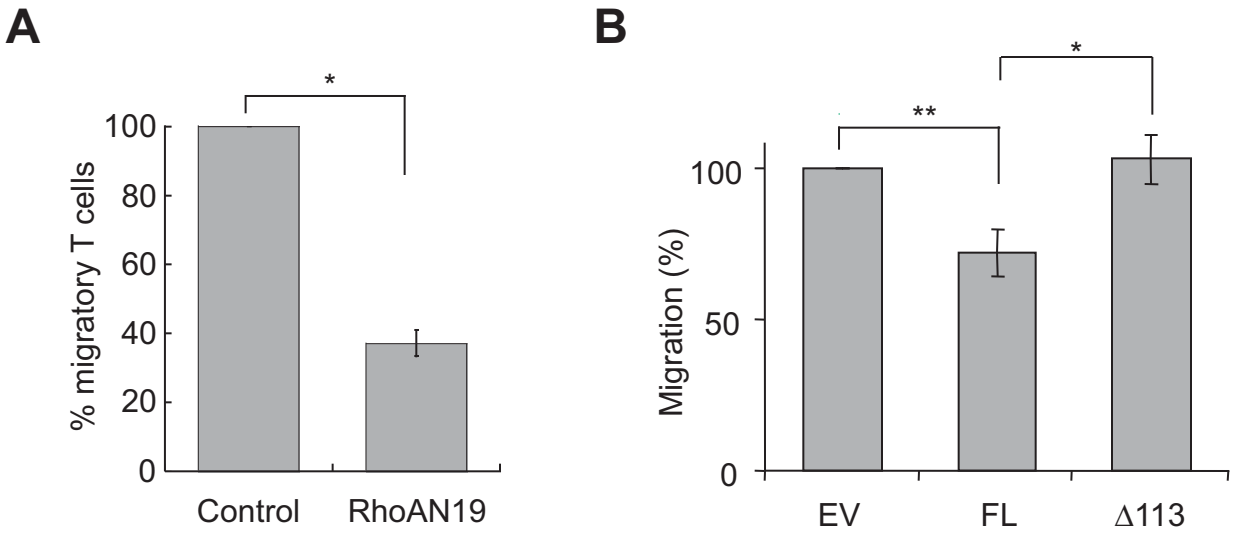
A
*
100
80
60
40
20
0
% migratory T cells
Control
RhoAN19
B
**
*
100
50
0
Migration (%)
EV
FL
Δ113

Figure 5

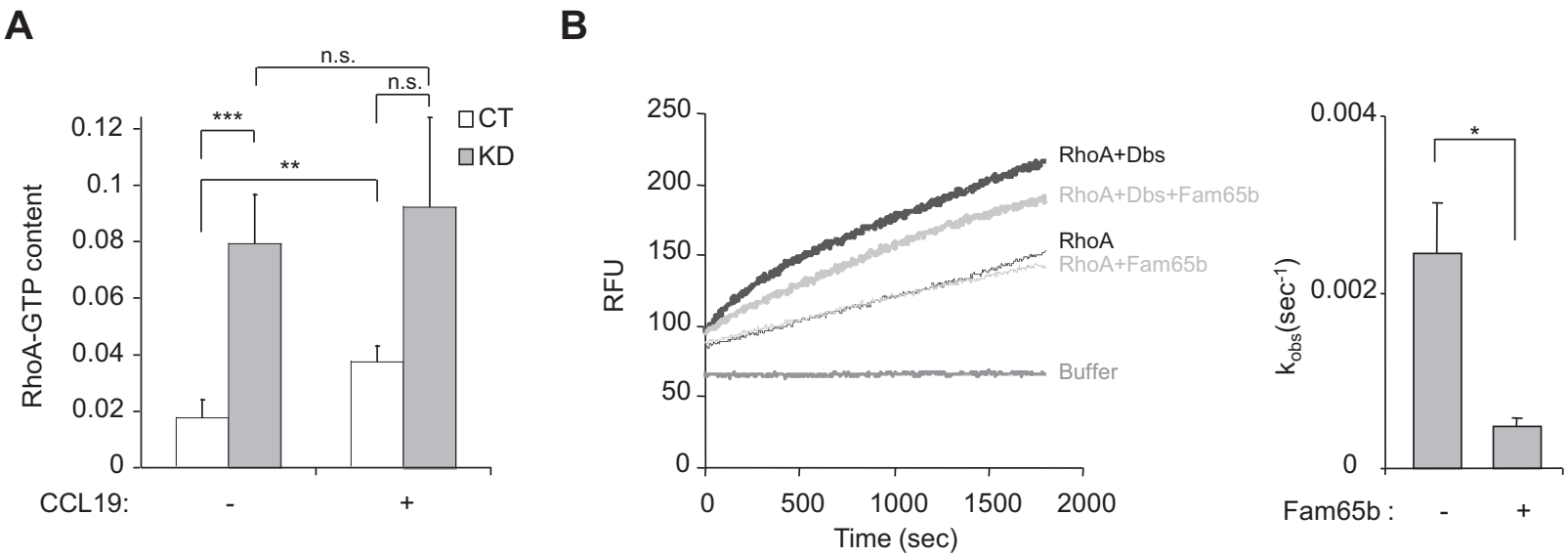
A
n.s.
n.s.
***
**
CT
KD
RhoA-GTP content
0.12
0.1
0.08
0.06
0.04
0.02
0
CCL19:
-
+
B
250
200
150
100
50
0
RFU
RhoA+Dbs
RhoA+Dbs+Fam65b
RhoA
RhoA+Fam65b
Buffer
0
500
1000
1500
2000
Time (sec)
0.004
0.002
0
$k_{obs}(sec^{-1})$
*
Fam65b :
-
+